Toluene Combustion: Reaction Paths, Thermochemical Properties, and Kinetic Analysis for the Methylphenyl Radical + O_2 Reaction

Gabriel da Silva, Chiung-Chu Chen, and Joseph W. Bozzelli*

Department of Chemistry and Environmental Science, New Jersey Institute of Technology, Newark, New Jersey 07102

Received: December 15, 2006; In Final Form: July 2, 2007

Aromatic compounds such as toluene and xylene are major components of many fuels. Accurate kinetic mechanisms for the combustion of toluene are, however, incomplete, as they do not accurately model experimental results such as strain rates and ignition times and consistently underpredict conversion. Current kinetic mechanisms for toluene combustion neglect the reactions of the methylphenyl radicals, and we believe that this is responsible, in part, for the shortcomings of these models. We also demonstrate how methylphenyl radical formation is important in the combustion and pyrolysis of other alkyl-substituted aromatic compounds such as xylene and trimethylbenzene. We have studied the oxidation reactions of the methylphenyl radicals with O_2 using computational ab initio and density functional theory methods. A detailed reaction submechanism is presented for the 2-methylphenyl radical + O_2 system, with 16 intermediates and products. For each species, enthalpies of formation are calculated using the computational methods G3 and G3B3, with isodesmic work reactions used to minimize computational errors. Transition states are calculated at the G3B3 level, yielding high-pressure limit elementary rate constants as a function of temperature. For the barrierless methylphenyl + O_2 and methylphenoxy + O association reactions, rate constants are determined from variational transition state theory. Multichannel, multifrequency quantum Rice−Ramsperger−Kassel (qRRK) theory, with master equation analysis for falloff, provides rate constants as a function of temperature and pressure from 800 to 2400 K and 1×10^{-4} to 1×10^{3} atm. Analysis of our results shows that the dominant pathways for reaction of the three isomeric methylphenyl radicals is formation of methyloxepinoxy radicals and subsequent ring opening to methyl-dioxo-hexadienyl radicals. The next most important reaction pathway involves formation of methylphenoxy radicals + O in a chain branching process. At lower temperatures, the formation of stabilized methylphenylperoxy radicals becomes significant. A further important reaction channel is available only to the 2-methylphenyl isomer, where 6-methylene-2,4-cyclohexadiene-1-one (*ortho*-quinone methide, *o*-QM) is produced via an intramolecular hydrogen transfer from the methyl group to the peroxy radical in 2-methylphenylperoxy, with subsequent loss of OH. The decomposition of *o*-QM to benzene + CO reveals a potentially important new pathway for the conversion of toluene to benzene during combustion. A number of the important products of toluene combustion proposed in this study are known to be precursors of polyaromatic hydrocarbons that are involved in soot formation. Reactions leading to the important unsaturated oxygenated intermediates identified in this study, and the further reactions of these intermediates, are not included in current aromatic oxidation mechanisms.

1. Introduction

Aromatic compounds are major constituents of transportation fuels, and understanding their combustion kinetics is important in the design of efficient engines and in the abatement of atmospheric pollution. Considerable work has been performed on the thermochemistry and kinetics of benzene combustion,[1] however, comparatively less work has been carried out on the kinetic modeling of other aromatic components of hydrocarbon fuels such as toluene, xylene, and ethylbenzene. Of all aromatic compounds, toluene is the most significant fuel component, and a reasonable volume of experimental work has been performed on this system.[2] Existing reaction mechanisms for toluene combustion describe normalized species profiles from flow reactor oxidation studies when reaction time is normalized to a set toluene conversion fraction.[3] However, strain rates in opposed flow flames and ignition delays in shock tube studies are not well predicted by any of the available models[4] without the inclusion of fitted or estimated rate parameters.

Studies on the combustion of benzene have shown that one of the important reactions at combustion temperatures is the formation of the phenyl radical and the subsequent reaction of this radical with species such as O_2. In contrast, the important paths under lower-temperature atmospheric conditions involve the addition of OH to benzene and subsequent reactions of the cyclohexadienyl radical with O_2 and other species.[1a,5] The reaction of phenyl with O_2 is especially significant due to the high concentration of O_2 in combustion chambers and the large well depth (ca. 50 kcal mol^{-1})[6] for formation of the phenylperoxy radical.

In toluene oxidation, the emphasis on oxidation kinetics has been placed on the reactions of the resonance-stabilized benzyl radical and not the methylphenyl radical because of the much weaker methyl carbon C−H bond (89.8 kcal mol^{-1})[7] versus

* Corresponding author. E-mail: bozzelli@njit.edu. Telephone: + 1 973 596 3459. Fax: +1 973 596 3586.

10.1021/jp068640x CCC: $37.00
Published on Web 08/16/2007

SCHEME 1: Formation of the 3-Methylbenzoxyl Radical from *m*-Xylene

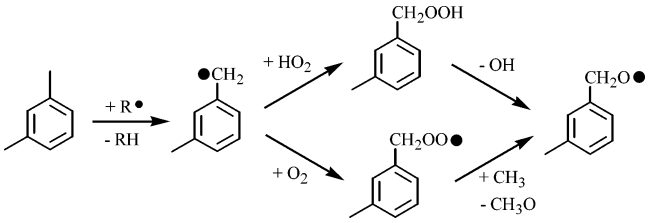

the phenyl C—H bond (112.9 kcal mol^{-1})[7] in toluene. While the benzyl radical is stable on a scale relative to other radicals, it does not react rapidly to new products in chemically activated association reactions with molecular oxygen; this is due to the low barrier (ca. 20 kcal mol^{-1}) and loose transition state for reverse reaction. In addition, the thermal decomposition of benzyl is slow, with an experimental activation energy of around 80 kcal mol^{-1}.[8]

Direct formation of the methylphenyl radical from toluene is less likely than formation of the benzyl radical because of the stronger phenyl carbon C—H bond dissociation energy. However, methylphenyl radicals do form during combustion and even in lower-temperature reactor cool-down zones by abstraction reactions with species in the active radical pool, and these abstraction reactions become more important at higher temperatures. The lifetime of the methylphenyl radicals will, however, be shorter at higher temperatures due to isomerization with the thermodynamically more stable benzyl radical via intramolecular hydrogen shift reactions.

While the benzyl radical may be the more stable and dominant C_7H_7 isomer in the reactions of toluene, there are several important pathways to methylphenyl radicals from poly-alkyl-substituted aromatics, including the xylenes and trimethyl benzenes. Experimental studies on the pyrolysis of toluene have identified two important initial pathways: benzyl + H formation and phenyl + CH_3 formation. The phenyl + CH_3 pathway constitutes around 20% of the total reaction rate at 1200 K and below but becomes the dominant pathway at temperatures of around 1800−2000 K.[9] In the high-temperature reactions of xylene and trimethyl benzene, we therefore expect methylphenyl and dimethylphenyl radical formation, via C—CH_3 bond dissociation, to be important. We also posit that methylphenyl radical formation will also be important at lower temperatures, due to indirect formation via the reactions of methylbenzyl radicals. In Scheme 1, we depict two processes leading to production of the methylbenzoxyl radical from xylene through chemically activated reactions of the 3-methylbenzyl radical with O_2 and HO_2 (similar reactions will occur for the 2- and 4-methylbenzyl isomers). The analogous benzyl + HO_2 reaction is fast, barrierless, and primarily forms benzoxyl radicals; the benzyl + HO_2 rate constant has been estimated as 5×10^{12} cm^3 mol^{-1} s^{-1}.[10] Once formed, methylbenzoxyl radicals can react via several pathways to produce methylphenyl radicals (among other products), as illustrated in Scheme 2. Here, reactions involving loss of hydrogen may proceed via either unimolecular dissociation or hydrogen abstraction reactions. The reactions of Scheme 2 result in methylphenyl radical formation at temperatures where isomerization with the benzyl radical is relatively unimportant, and a study to further quantify these reaction paths would be of considerable value.

The above discussion illustrates that the reactions of the methylphenyl radical, and of substituted methylphenyl radicals, need to be incorporated into aromatic oxidation mechanisms.

SCHEME 2: Methylphenyl Radical Formation from the 3-Methylbenzoxyl Radical

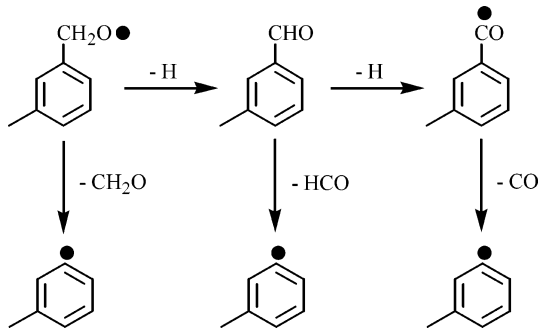

This includes the important reactions of these radicals with O_2. In this study, we focus on the initial reactions in the methylphenyl radical + O_2 system. Thermochemical properties and elementary rate constants are calculated for species and reactions involved in this relatively complex reaction system using the G3 and G3B3 composite theoretical methods. A submechanism is compiled for the methylphenyl + O_2 reaction, and rate constants are calculated as a function of temperature and pressure for the chemical activation system and for dissociation of stabilized intermediates, where the barrierless methylphenyl + O_2 and methylphenoxy + O reactions are treated using variational transition state theory. It is hoped that this study will provide kinetic and thermochemical input for the construction of reaction models for the combustion and oxidation of toluene, the xylenes, and other (poly)-alkyl-substituted aromatics, while also identifying important intermediate species in these systems that need additional study.

2. Methods

2.2. Computational Methods. All calculations were made using the Gaussian 03 suite of programs.[11] The composite theoretical methods G3[12] and G3B3[13] were applied to all potential energy minima identified in the 2-methylphenyl radical + O_2 reaction mechanism, while the G3B3 method was applied to all transition states. Transition states were identified by their single imaginary frequency, whose mode of vibration connects the reactants and products. For equilibrium geometries, enthalpies of formation were calculated from atomization enthalpies, as well as from isodesmic reaction enthalpies. For transition states, enthalpies of formation were obtained from the computational enthalpy of activation and from the calculated enthalpies of formation of the reactants or products. Calculated geometries (in Cartesian coordinates) and enthalpies (in hartrees) for all molecules, including transition states, are provided as Supporting Information.

The composite theoretical technique G3 involves an initial HF/6-31G(d) level geometry optimization and frequency calculation, followed by a further geometry optimization at the MP2/6-31G(d) level of theory. In the G3B3 method, these initial steps are replaced by a B3LYP/6-31G(d) geometry optimization and frequency calculation. The final MP2 and B3LYP geometries from both methods are subjected to a series of QCISD(T), MP4, and MP2 level energy corrections to accurately determine the molecular energy. The theoretical methods G3 and G3B3 provide a good compromise between accuracy and computational efficiency for the relatively large system being studied here (9 heavy atoms). For small closed-shell organic molecules, the G3 and G3B3 methods calculate thermochemical properties with an average uncertainty of around 1 kcal mol^{-1},

with G2 test set root-mean-square errors of ± 0.9 and ± 1.0 kcal mol^{-1}, respectively. However, these methods are expected to be somewhat less accurate for the larger radical molecules in our reaction system, due principally to greater systematic computational errors and the effects of spin contamination. For radical species, both the G3 and G3B3 methods will suffer from spin contamination correction errors; these errors will be greatest for the MP2 and HF level calculations. Comparatively, the B3LYP density functional, which is utilized in the G3B3 method, is much less susceptible to spin contamination than HF methods.[14] In this study, isodesmic work reactions are used when evaluating enthalpies of formation, for error cancellation and help in mitigation of spin contamination, and other systematic computational errors.

2.3. Entropy ($S°_{298}$) and Heat Capacity ($C_P(T)$) Calculations. The entropy (298 K) and heat capacity (300−1500 K) of each molecule is calculated from principles of statistical mechanics using the SMCPS program,[15] with B3LYP/6-31G(d) geometries, frequencies, and moments of inertia. SMCPS applies the rigid-rotor-harmonic-oscillator (RRHO) approximation, with the required entropy corrections for unpaired electrons, symmetry, and optical isomers. Low-frequency vibrational modes corresponding to internal molecular rotations are omitted from the SMCPS calculations, and appropriate entropy and heat capacity corrections are added. Internal rotor potentials were calculated for rotation about R−CH_3 and R−$OO^•$ bonds at the B3LYP/6-31G(d,p) level of theory with the 2-methylphenyl and 2-methylphenylperoxy radicals, respectively. Rotor potentials were fit to five-parameter Fourier series expansions, and the program ROTATOR was then used to determine the $S°_{298}$ and $C_P(T)$ corrections.[16] Internal rotation corrections for molecules containing the groups phenyl−OH,[17] phenyl−O−OH,[6] and phenyl−O−O−CH_3[18] were obtained from the literature. All internal rotor corrections, and calculated R−OO and R−CH_3 rotor potentials in 2-methylphenyl and 2-methylphenylperoxy, are provided in the Supporting Information. Frequencies and moments of inertia for all ground and transition state molecules are also provided as Supporting Information.

2.4. Reaction Rate Parameters and Kinetic Analysis. Rate constants, $k(T)$, were calculated as a function of temperature from activation enthalpies and entropies via canonical transition state theory and statistical mechanics (eq 1) in the temperature range of 300−2000 K. In eq 1, $\Delta S^‡$ is the activation entropy, $\Delta H^‡$ is the activation enthalpy, k_B is the Boltzmann constant, and h is the Planck constant. Observe in eq 1 that the activation entropy is a function of temperature; we calculate the change in entropy with temperature from the integral of $C_P(T)$ with respect to log T.

$$k(T) = \frac{k_B T}{h} \exp\left(\frac{\Delta S^‡(T)}{R}\right) \exp\left(\frac{-\Delta H^‡}{RT}\right) \quad (1)$$

Rate constants for reactions featuring an intramolecular hydrogen shift are corrected for the effects of quantum mechanical tunneling using the Wigner formalism (eq 2),[19] where $\kappa(T)$ is the tunneling correction, $\upsilon^‡$ is the transition state's imaginary vibrational frequency, k_B is the Boltzmann constant, and h is the Planck constant.

$$\kappa(T) = 1 + \frac{1}{24}\left(\frac{h\upsilon^‡}{k_B T}\right) \quad (2)$$

Calculated $k(T)$ values were fit to an empirical three-parameter form of the Arrhenius equation (eq 3) to obtain the rate parameters A' and n, where E_a was fixed to the 298 K activation enthalpy. Where multiple degenerate sites were available for reaction (i.e., abstraction of H from CH_3), the pre-exponential factor (A') was multiplied by the appropriate factor.

$$k(T) = A'T^n \exp\left(\frac{-E_a}{RT}\right) \quad (3)$$

Saddle-point transition states were not located for dissociation of the methylphenylperoxy radical to either the methylphenyl radical + O_2 or the methylphenoxy radical + O at the B3LYP/6-31G(d) level. These barrierless reactions have been treated according to variational transition state theory from O3LYP/6-31G(d) scans of the potential energy surface.[20] The results of these calculations are the subject of a forthcoming publication. Additionally, a saddle-point transition state was located for the 2-hydroxy-6-methylphenoxy → 3-methyl-1,2,-benzoquinone + H reaction, but the G3B3 enthalpy of the transition state was also below the enthalpy of the products; this reaction was assumed to proceed with $E_a = 0$ in the reverse direction.

Temperature- and pressure-dependent rate constants for reactions of the chemically activated methylphenylperoxy adduct were calculated with multichannel, multifrequency quantum Rice−Ramsperger−Kassel (qRRK) theory for $k(E)$[15,21,22] and master equation analysis for falloff and stabilization.[15,22] Elementary rate parameters (A', n, and E_a) for the elementary reaction steps were calculated as described above. The qRRK calculations were performed using the program CHEMASTER[15,22] for $T = 800-2400$ K and $P = 1 \times 10^{-4}$ to 1×10^3 atm. The CHEMASTER code is used with energy levels from a full set of $3n-6$ vibrational frequencies, but in a reduced form of three representative frequencies that accurately reproduce the heat capacity versus temperature curve[23] plus energy levels from one external rotation. The qRRK/master equation analysis has been shown to accurately reproduce both experimental[21,22] and Rice−Ramsperger−Kassel−Marcus (RRKM) results.[24] Unimolecular isomerization and dissociation kinetics of the stabilized methylphenylperoxy radical is also included by using the CHEMDIS program.[21] Molecules that pass over a transition state, where there are subsequent barriers to other new channels, are treated as chemically activated and considered in the program for possible further reaction(s).

3. Results and Discussion

3.1. Thermochemical Parameters and Error Analysis. Table 1 illustrates the structure of the 2-methylphenyl radical and the stable intermediates on the 2-methylphenyl + O_2 potential energy surface. Enthalpies of formation for these 16 species have been calculated using a series of 2−4 isodesmic reactions with the G3 and the G3B3 methods. The isodesmic reaction schemes are provided in Table 2, along with the calculated reaction enthalpies for each reaction, while specific enthalpies of formation calculated with each reaction are provided in the Supporting Information. Experimental enthalpies of formation for all reference species in our isodesmic work reactions are listed in Table 3. The use of isodesmic work reaction schemes when calculating enthalpies of formation and bond dissociation energies can increase computational accuracy due to the cancellation of systematic calculation errors.[33,39,40] Typical uncertainties in high-level composite computational theoretical methods with implementation of isodesmic work reactions are reduced from around 1 kcal mol^{-1} to around 0.5 kcal mol^{-1} [33,40] provided that accurate experimental enthalpies are available for the work reaction reference species.

In developing the isodesmic work reactions, efforts were made to preserve the bonding environment in the target species,

TABLE 1: Structures and Names for All Species Studied on the 2-Methylphenyl Radical + O_2 Potential Energy Surface

structure	name	structure	name
	(1) 2-methylphenyl	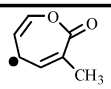	(9) 7-methyloxepinoxy
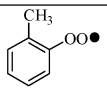	(2) 2-methylphenylperoxy	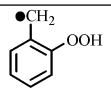	(10) 2-phenylhydroperoxy -1-methylene
	(3) 4-dioxirane-5-methyl -2,5-cyclohexadienyl radical		(11) *ortho*-quinone methide
	(4) 2-methylphenoxy		(12) 4-methyl-5,6-dioxetane -2,4-cyclohexadienyl
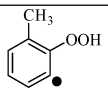	(5) 3-methyl-2-hydroperoxyphenyl	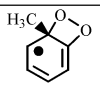	(13) 6-methyl-5,6-dioxetane -2,4-cyclohexadienyl
	(6) 2-hydroxy-6-methyl-phenoxy	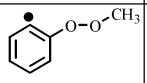	(14) 2-methylperoxyphenyl
	(7) 3-methyl-1,2-benzoquinone		(15) 6-methyl-1,6-dioxo -2,4-hexadienyl
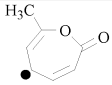	(8) 3-methyloxepinoxy		(16) 2-methyl-1,6-dioxo -2,4-hexadienyl

including aromaticity and ring structure, so as to effectively cancel errors in bond energies and adjacent interaction energies across the work reactions. In addition, each isodesmic reaction typically features the same number of radical species, internal rotors, and molecular fragments on either side of the reaction, helping eliminate errors due to spin contamination, hindered internal rotation, and basis set superposition error, respectively. In many instances, vinylic groups were used to model bonds in aromatic molecules, as it has been demonstrated that bonds in similar aromatic and vinyl molecules are close in energy.[17,41] Reaction enthalpies for the isodesmic work reactions were typically small (on average 29 kcal mol^{-1}), which indicates that there is good cancellation of bond energy across the reactions.

The enthalpies of formation calculated with our isodesmic reaction schemes are given in Table 4. Also included in Table 4 are enthalpies of formation calculated from atomization enthalpies. The lack of error cancellation in atomization reactions makes these enthalpies generally less accurate than isodesmic enthalpies, although the atomization values have the advantage of using the well-known enthalpies of formation of the atoms C, O, and H. We recommend an average of the G3 and G3B3 isodesmic enthalpies as the best values, and we use these enthalpies in our qRRK/master equation calculations (this is justified below). We note that, in general, the enthalpies calculated with both theoretical methods are in good agreement, although there are relatively significant differences (>2 kcal mol^{-1}) between the G3 and G3B3 enthalpies for the 2-methylphenylperoxy and 6-methyl-1,6-dioxo-2,4-hexadienyl radicals. The average difference between the isodesmic and atomization enthalpies is 1 kcal mol^{-1}. We note that literature enthalpy values, either experimental or computational, with which to compare our calculated enthalpies of formation could not be located for any oxy-hydrocarbon radicals in this study.

The error associated with enthalpies of formation calculated via isodesmic work reactions will consist of two components: (i) the intrinsic error associated with the computational method (the computational error), and (ii) the error associated with the experimental enthalpies of formation of the reference species in the work reaction (the experimental error). We have estimated the intrinsic computational error component from the standard deviation for enthalpies of formation calculated using different isodesmic work reactions across the two theoretical methods. This approach is justified given the large number of work reactions (50 in total) and the use of multiple theoretical methods. Averaged over all 16 compounds, we obtain a standard deviation of 0.87 kcal mol^{-1}, with maximum standard deviation of 1.5 kcal mol^{-1}. For the computational error component we suggest a 95% confidence interval uncertainty of $\pm$1.7 kcal mol^{-1}, which is twice the standard deviation. The second error component, which arises due to uncertainty in the reference enthalpies, was evaluated for each isodesmic reaction as the quadratic mean (root-mean-square) of the uncertainties for all reference species in the work reaction. For each species, the reaction with the largest uncertainty then provides the experimental error. The total uncertainty for each species is calculated as the quadratic mean of the computational error and the experimental error. The average total uncertainty is found to be $\pm$1.9 kcal mol^{-1}, while the maximum uncertainty is $\pm$2.3 kcal mol^{-1}. Recommended enthalpies of formation, with uncertainties, are included in Table 5. These values are also provided as Supporting Information, along with the computational and experimental contributions to the total uncertainty. Given that the computational error is evaluated as 1.7 kcal mol^{-1}, our error analysis indicates that uncertainties in the experimental enthalpies of formation of the reference species contributes relatively little to the overall error, and the enthalpies

TABLE 2. Isodesmic Work Reactions and Reaction Enthalpies Calculated with the G3B3 and G3 Theoretical Methods

species[a]	work reaction	$\Delta_{rxn}H°_{298}$ (kcal mol^{-1}) G3B3	G3
(1)	(1) + CH_2=CH_2 → toluene + CH_2=CH	−4.2	−4.3
	(1) + 2 CH_2=CH_2 → benzene + CH_2=CH + propene	−3.8	−3.9
	(1) + 2 CH_2=CH_2 + C_2H_6 → benzene + CH_2=CH + CH_4 + 1-butene	−6.3	−6.4
(2)	(2) + H_2O → 2-methylphenol + HOO	2.2	4.7
	(2) + H_2O + CH_2=CH_2 → phenol + propene + HOO	3.3	5.8
	(2) + H_2O + CH_2=CH_2 + C_2H_6 → phenol + 1-butene + CH_4 + HOO	0.8	3.3
(3)	(3) + $3CH_4$ + $2H_2O$ → 1,3-cyclohexadiene + $2CH_3OH$ + H_2O_2 + CH_3CH_2	55.9	57.7
	(3) + $3CH_4$ + $2H_2O$ → 1,4-cyclohexadiene + $2CH_3OH$ + H_2O_2 + CH_3CH_2	56.0	57.9
(4)	(4) + H_2O_2 → 2-methylphenol + HOO	−0.1	0.2
	(4) + H_2O_2 + CH_2=CH_2 → phenol + propene + HOO	1.0	1.3
	(4) + H_2O_2 + CH_2=CH_2 + C_2H_6 → phenol + 1-butene + CH_4 + HOO	−1.5	−1.2
(5)	(5) + CH_3OH + CH_2=CH_2 → 2-methylphenol + CH_2=CH + CH_3OOH	−9.9	−10.0
	(5) + H_2O + CH_2=CH_2 → 2-methylphenol + CH_2=CH + H_2O_2	−1.9	−1.9
	(5) + H_2O + 2 CH_2=CH_2 → phenol + propene + CH_2=CH + H_2O_2	−0.8	−0.8
	(5) + H_2O + CH_2=CH_2 + C_2H_6 → phenol + 1-butene + CH_2=CH + H_2O_2 + CH_4	−3.3	−3.3
(6)	(6) + CH_2=CH_2 + H_2O_2 → 1,3-benzenediol + propene + HOO	9.7	9.8
	(6) + CH_2=CH_2 + C_2H_6 + H_2O_2 → 1,3-benzenediol + 1-butene + CH_4 + HOO	7.3	7.3
	(6) + CH_2=CH_2 + C_3H_8 + H_2O_2 → 1,3-benzenediol + 1-butene + C_2H_6 + HOO	10.0	10.0
(7)	(7) + CH_2=CH_2 + $2CH_4$ → 1,3-cyclohexadiene + $2H_2C$=O + propene	32.0	32.4
	(7) + CH_2=CH_2 + $2CH_4$ → 1,4-cyclohexadiene + $2H_2C$=O + propene	32.1	32.6
	(7) + C_2H_6 + $2CH_4$ → 1,3-cyclohexadiene + $2H_2C$=O + C_3H_8	34.6	35.1
	(7) + C_2H_6 + $2CH_4$ → 1,4-cyclohexadiene + $2H_2C$=O + C_3H_8	34.7	35.3
(8)	(8) + H_2O + $3CH_4$ → 1,3-cyclohexadiene + $2CH_3OH$ + H_2C=O + CH_3	73.9	75.2
	(8) + H_2O + $3CH_4$ → 1,4-cyclohexadiene + $2CH_3OH$ + H_2C=O + CH_3	74.0	75.4
	(8) + H_2O + $2CH_4$ + C_2H_6 → 1,3-cyclohexadiene + $2CH_3OH$ + H_2C=O + CH_3CH_2	70.6	72.2
	(8) + H_2O + $2CH_4$ + C_2H_6 → 1,4-cyclohexadiene + $2CH_3OH$ + H_2C=O + CH_3CH_2	70.7	72.4
(9)	(9) + H_2O + $3CH_4$ → 1,3-cyclohexadiene + $2CH_3OH$ + H_2C=O + CH_3	71.3	72.6
	(9) + H_2O + $3CH_4$ → 1,4-cyclohexadiene + $2CH_3OH$ + H_2C=O + CH_3	71.4	72.9
	(9) + H_2O + $2CH_4$ + C_2H_6 → 1,3-cyclohexadiene + $2CH_3OH$ + H_2C=O + CH_3CH_2	68.0	69.6
	(9) + H_2O + $2CH_4$ + C_2H_6 → 1,4-cyclohexadiene + $2CH_3OH$ + H_2C=O + CH_3CH_2	68.1	69.8
(10)	(10) + CH_3OH + CH_4 → 2-methylphenol + CH_3OOH + CH_3	7.0	7.9
	(10) + H_2O + CH_4 → 2-methylphenol + CH_3 + H_2O_2	15.1	16.0
	(10) + OH + CH_4 → 2-methylphenol + CH_3 + HOO	−15.9	−15.2
(11)	(11) + $2CH_4$ → 1,3-cyclohexadiene + H_2C=O + CH_2=CH_2	34.8	35.2
	(11) + $2CH_4$ → 1,4-cyclohexadiene + H_2C=O + CH_2=CH_2	34.8	35.4
(12)	(12) + $3CH_4$ + $2H_2O$ → 1,3-cyclohexadiene + $2CH_3OH$ + H_2O_2 + CH_3CH_2	30.3	32.1
	(12) + $3CH_4$ + $2H_2O$ → 1,4-cyclohexadiene + $2CH_3OH$ + H_2O_2 + CH_3CH_2	30.4	32.3
(13)	(13) + $3CH_4$ + $2H_2O$ → 1,3-cyclohexadiene + $2CH_3OH$ + H_2O_2 + CH_3CH_2	33.2	35.2
	(13) + $3CH_4$ + $2H_2O$ → 1,4-cyclohexadiene + $2CH_3OH$ + H_2O_2 + CH_3CH_2	33.3	35.4
(14)	(14) + H_2O + CH_2=CH_2 → phenol + CH_3OOH + CH_2=CH	−1.0	−0.8
	(14) + $2H_2O$ + CH_2=CH_2 → phenol + H_2O_2 + CH_3OH + CH_2=CH	7.1	7.3
	(14) + $2H_2O$ + propene → 2-methylphenol + H_2O_2 + CH_3OH + CH_2=CH	6.1	6.2
(15)	(15) + CH_4 + CH_2=CH_2 + C_2H_6 → 1,3-cyclohexadiene + $2H_2C$=O + propene + CH_3	40.6	39.5
	(15) + CH_4 + CH_2=CH_2 + C_2H_6 → 1,4-cyclohexadiene + $2H_2C$=O + propene + CH_3	40.7	39.7
	(15) + CH_4 + CH_2=CH_2 + C_3H_8 → 1,3-cyclohexadiene + $2H_2C$=O + propene + CH_3CH_2	40.0	39.1
	(15) + CH_4 + CH_2=CH_2 + C_3H_8 → 1,4-cyclohexadiene + $2H_2C$=O + propene + CH_3CH_2	40.1	39.3
(16)	(16) + CH_4 + CH_2=CH_2 + C_2H_6 → 1,3-cyclohexadiene + $2H_2C$=O + propene + CH_3	37.8	38.2
	(16) + CH_4 + CH_2=CH_2 + C_2H_6 → 1,4-cyclohexadiene + $2H_2C$=O + propene + CH_3	37.9	38.4
	(16) + CH_4 + CH_2=CH_2 + C_3H_8 → 1,3-cyclohexadiene + $2H_2C$=O + propene + CH_3CH_2	37.2	37.8
	(16) + CH_4 + CH_2=CH_2 + C_3H_8 → 1,4-cyclohexadiene + $2H_2C$=O + propene + CH_3CH_2	37.3	39.3

[a] See Table 1 for species identification.

of formation calculated using the isodesmic approach should therefore offer considerable improvements in accuracy over the enthalpies from atomization calculations.

The entropy and heat capacity of each species has been calculated using the statistical mechanics program SMCPS, with B3LYP/6-31G(d) geometries, frequencies, and moments of inertia. Where an internal rotor was present, the torsion vibrational frequency was removed from the statistical mechanics analysis, and the $S°_{298}$ and $C_P(T)$ contributions replaced with contributions from a hindered rotor analysis. Table 5 presents the standard entropy for each species and the heat capacity at 300−1500 K, along with the recommended value for the standard enthalpy of formation.

3.2. Kinetic Parameters. Scheme 3 illustrates the proposed reaction pathways in the 2-methylphenyl + O_2 reaction system. Transition states have been calculated for each reaction identified on the 2-methylphenyl + O_2 potential energy surface, and the geometry of each transition state is depicted in Figure 1. Transition state numbering in Figure 1 is defined in Figure 2. Enthalpies of formation, entropies, and heat capacities are

TABLE 3: Literature Enthalpies of Formation (kcal mol^{-1}) Used in Isodesmic Enthalpy Calculations

	$\Delta_f H°_{298}$	ref
CH_4	-17.89 ± 0.1	25
C_2H_6	-20.24 ± 0.12	26
C_3H_8	-24.82 ± 0.14	26
benzene	19.82 ± 0.12	27
toluene	11.95 ± 0.15	27
CH_3	34.821 ± 0.2	25
CH_3CH_2	28.4 ± 0.5	28
CH_3OH	-48.07 ± 0.05	29
H_2O_2	-32.531 ± 0.05	25
CH_3OOH	-31.31 ± 1.2	30
OH	9.319 ± 0.03	25
H_2O	-57.799 ± 0.01	25
1,4-cyclohexadiene	26.1 ± 0.14	31
1,3-cyclohexadiene	25.00 ± 0.15	32
$H_2C{=}O$	-26.05 ± 0.42	33
CH2═CH	71.0 ± 1	28
CH2═CH2	12.54 ± 0.1	25
propene	4.879 ± 0.16	34
1-butene	-0.15 ± 0.19	35
2-methylphenol	-30.67 ± 0.21	36
phenol	-23.03 ± 0.14	36
HOO	2.94 ± 0.06	37
1,3-benzenediol	-65.7 ± 0.29	38

TABLE 4: Enthalpies of Formation ($\Delta_f H°_{298}$, kcal mol^{-1}) for Species Involved in the 2-Methylphenyl Radical + O_2 Reaction Mechanism, Calculated from Isodesmic and Atomization Work Reactions

	isodesmic		atomization	
	G3B3	G3	G3B3	G3
2-methylphenyl	74.4	74.5	75.2	75.4
2-methylphenylperoxy	27.1	24.6	28.5	26.1
4-dioxirane-5-methyl-2,5-cyclohexadienyl	38.6	36.7	40.2	39.8
2-methylphenoxy	4.1	3.8	5.0	4.5
3-methyl-2-hydroperoxyphenyl	54.2	54.3	55.6	56.3
2-hydroxy-6-methylphenoxy	−47.9	−48.0	−46.3	−46.5
3-methyl-1,2-benzoquinone	−30.2	−30.7	−30.7	−29.8
3-methyloxepinoxy	−24.7	−26.2	−24.8	−25.1
7-methyloxepinoxy	−22.1	−23.6	−22.2	−22.5
2-phenylhydroperoxy-1-methylene	31.9	31.0	32.8	32.4
ortho-quinone methide	13.0	12.5	13.2	13.7
4-methyl-5,6-dioxetane-2,4-cyclohexadienyl	64.2	62.3	65.8	65.4
6-methyl-5,6-dioxetane-2,4-cyclohexadienyl	61.3	59.2	63.0	62.3
2-methylperoxyphenyl	63.5	63.4	64.5	65.1
6-methyl-1,6-dioxo-2,4-hexadienyl	−2.5	−1.6	−2.8	−0.7
2-methyl-1,6-dioxo-2,4-hexadienyl	0.3	−0.6	0.0	0.6

calculated for each transition state and are provided in Table 6. The kinetic parameters E_a, A', and n were determined for each reaction, as discussed in Section 2.4, and are listed here in Table 7. Literature values were not located for any of our calculated elementary rate parameters.

3.3. Reaction System. Figure 2 shows the potential energy diagram for the 2-methylphenyl + O_2 reaction system. This diagram features seven unique reaction pathways for the chemically activated 2-methylphenylperoxy adduct. These pathways are discussed below.

I. Stabilization of the Methylphenylperoxy Radical. This reaction will be important at lower temperatures for atmospheric and higher pressures. The methylphenyl + O_2 association results in a chemically activated methylphenylperoxy radical with a 48.6 kcal mol^{-1} well depth at 298 K. The methylphenylperoxy adduct is formed with no barrier and a loose transition state.[20] This energized adduct can react to new isomers, to new dissociation products (methylphenoxy + O), react back to methylphenyl + O_2, or be stabilized by collision(s) with the bath gas. The important rate constant for formation of the methylphenylperoxy radical, and for reverse dissociation to methylphenyl + O_2, has been treated by variational transition state theory.

II. Intramolecular Hydrogen Abstraction from the Methyl Group in the Methylphenylperoxy Radical by the Radical Peroxy Oxygen Atom (TS4). This reaction forms a resonantly stabilized hydroperoxide benzyl radical. This is the lowest-energy intermediate available to the 2-methylphenylperoxy radical, while the reaction proceeds with a low barrier of 26.5 kcal mol^{-1} (22.1 kcal mol^{-1} below the entrance channel). This benzylic radical is unstable and rapidly dissociates to *ortho*-quinone methide + OH (TS11) with a small activation energy (7.6 kcal mol^{-1}, or 35.5 kcal mol^{-1} below methylphenyl + O_2). This intramolecular reaction sequence is an important path that is not present in the combustion of benzene due to the involvement of the methyl group. To our knowledge, this reaction pathway has not been previously included in toluene and other alkyl-benzene combustion models.

For the *meta*- and *para*-methylphenyl systems, the out-of-plane ring bending in the transition state increases the activation energy such that this path is not competitive. Furthermore, for the *meta*-methylphenyl system, the stable quinone methide is not formed as for the ortho and para isomers because the product cannot yield the stabilizing cyclohexadiene structure. This should make the OH dissociation step endothermic, increasing the activation energy and thus making this pathway unfavorable.

III. Formation of the 2-Hydroxy-6-methylphenoxy Radical. This occurs via a two step process: (i) formation of a hydroperoxide methylphenyl radical by intramolecular hydrogen transfer of the *ortho*-phenyl hydrogen in the 2-methylphenylperoxy adduct (TS3), and (ii) a subsequent intramolecular OH shift (TS10). To our knowledge, this reaction path has not been considered in previous studies of aromatic systems. Intramolecular hydrogen abstraction from the ortho position in the 2-methylphenyl radical is found to have a barrier that is 4 kcal mol^{-1} below the entrance channel and may therefore have some importance. The 3-methyl-2-hydroperoxyphenyl radical can undergo an ortho OH shift, forming a product with over 100 kcal mol^{-1} of chemical activation energy. If formed, this energized radical has sufficient energy to undergo unimolecular dissociation to several plausible product sets, with dissociation to 3-methyl-1,2-benzoquinone + H illustrated. This methylbenzoquinone product retains a fraction of the chemical activation energy and can undergo cleavage of the relatively weak C(═O)—C(═O) bond, forming a dicarbonyl ring-opening product.

IV. Dissociation of the Methylphenylperoxy Radical to Give the Methylphenoxy Radical + O (TS5). This reaction proceeds with an activation energy equal to its reaction enthalpy, which is ca. 11 kcal mol^{-1} below the 2-methylphenyl + O_2 entrance channel. This reaction has a loose transition-state structure, with cleavage of the RO—O$^{\bullet}$ bond and formation of a near-double C═O bond, and has a negligible barrier for reverse reaction. This important dissociation of the methylphenylperoxy adduct is a chain branching reaction, forming a phenoxy radical and an oxygen atom. This barrierless reaction is treated variationally.

V. Ipso Addition of the Peroxy Radical to the Aromatic Ring (TS2). This reaction is important because of its low barrier (21.1 kcal mol^{-1}) and was first identified by Carpenter[1h] in the phenyl + O_2 reaction system. The peroxy radical adds at the ipso position to form a dioxirane-methylcyclohexadienyl radical, with a barrier ca. 28 kcal mol^{-1} below the entrance channel. The

TABLE 5: Recommended Enthalpies ($\Delta_f H°_{298}$), Entropies ($S°_{298}$), and Heat Capacities ($C_P(T)$) for Species Involved in the Methylphenyl Radical + O_2 Combustion Mechanism[a]

species[b]	$\Delta_f H°_{298}$	$S°_{298}$	$C_{P,300}$	$C_{P,400}$	$C_{P,500}$	$C_{P,600}$	$C_{P,800}$	$C_{P,1000}$	$C_{P,1500}$
2-methylphenyl	74.5 ± 2.0	81.17	23.97	31.63	38.33	43.85	52.15	57.98	66.70
2-methylphenylperoxy	25.8 ± 1.8	92.14	31.82	41.07	48.62	54.50	62.86	68.56	76.99
4-dioxirane-5-methyl-2,5-cyclohexadienyl	37.7 ± 1.8	90.03	31.58	40.62	48.18	54.27	63.17	69.31	78.33
2-methylphenoxy	3.9 ± 1.8	85.86	27.53	35.77	42.88	48.71	57.39	63.44	72.40
3-methyl-2-hydroperoxyphenyl	54.2 ± 2.3	98.06	32.25	40.60	47.72	53.49	62.00	67.86	76.43
2-hydroxy-6-methylphenoxy	−47.9 ± 1.8	88.64	31.80	40.93	48.41	54.34	62.95	68.86	77.56
3-methyl-1,2-benzoquinone	−30.5 ± 1.9	89.06	30.36	38.20	44.94	50.51	58.87	64.69	73.23
3-methyloxepinoxy	−25.4 ± 1.9	91.85	31.39	40.08	47.47	53.52	62.52	68.79	78.04
7-methyloxepinoxy	−22.8 ± 1.9	91.52	31.31	39.99	47.40	53.46	62.48	68.76	78.04
2-phenylhydroperoxy-1-methylene	31.4 ± 2.1	92.72	33.44	42.45	49.76	55.50	63.74	69.36	77.60
ortho-quinone methide	12.8 ± 1.8	79.75	27.04	35.00	41.67	47.05	54.99	60.49	68.59
4-methyl-5,6-dioxetane-2,4-cyclohexadienyl	63.3 ± 1.8	91.55	31.10	40.12	47.75	53.91	62.98	69.22	78.34
6-methyl-5,6-dioxetane-2,4-cyclohexadienyl	60.3 ± 1.8	89.75	31.24	40.52	48.20	54.33	63.24	69.36	78.35
2-methylperoxyphenyl	63.4 ± 2.3	98.93	31.78	40.33	47.53	53.40	62.05	68.09	76.98
6-methyl-1,6-dioxo-2,4-hexadienyl	−2.1 ± 1.9	98.30	34.60	42.55	49.29	54.83	63.23	69.20	78.20
2-methyl-1,6-dioxo-2,4-hexadienyl	−0.2 ± 1.9	99.39	34.36	41.99	48.67	54.27	62.85	68.98	78.15

[a] Geometries, frequencies and moments of inertia from B3LYP/6-31G(d) calculations. Enthalpies in kcal mol^{-1}, entropies and heat capacities in cal mol^{-1} K^{-1}. [b] See Table 1 for species identification

SCHEME 3: Proposed Reaction Pathways in the 2-Methylphenyl + O_2 Reaction System

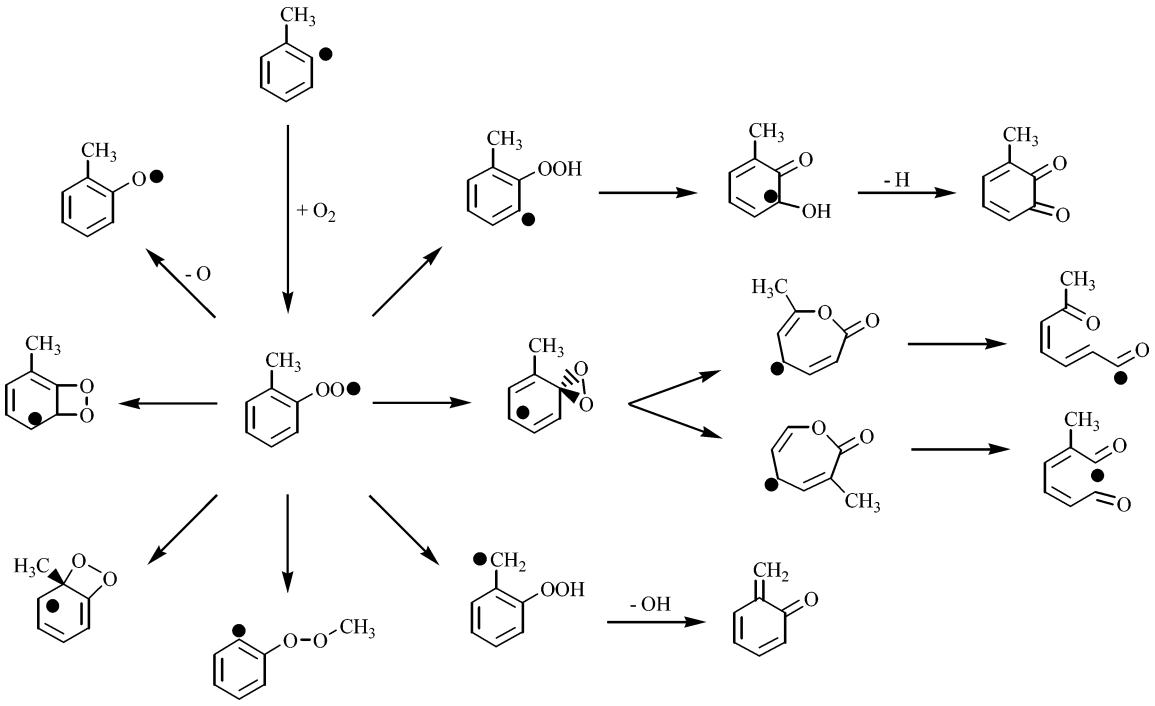

dioxirane-methylcyclohexadienyl radical exists in a shallow well, with forward (TS9) and reverse (TS2) barriers both less than 15 kcal mol^{-1} and over 20 kcal mol^{-1} below the entrance channel energy. Forward reaction of this dioxirane radical results in formation of the 3- and 7-methyl-oxepinoxy radicals, which both lie some 80 kcal mol^{-1} below the barrier from the dioxirane-methylcyclohexadienyl radical. Ring-opening reactions of these methyloxepinoxy radicals (TS13 and TS14) have barriers that are around 74 kcal mol^{-1} below the methylphenyl + O_2 entrance level. Accordingly, once formed, the methyloxepinoxy radicals will show little or no reverse reaction or stabilization; they undergo ring opening instead. The ring-opening reactions of the methyloxepinoxy adducts to form 2- and 6-methyl-1,6-dioxo-2,4-hexadienyl have barriers of ca. 25 kcal mol^{-1}. These ring-opening products will follow two general paths: (a) a sequence of bond dissociation reactions, leading, eventually, to small-chain unsaturated hydrocarbons and oxyhydrocarbons, and (b) ring-closure reactions to low-energy five- and six-membered oxyhydrocarbons. These two general pathways are similar to those of the oxepinoxy radical,[1d,e,42] which is formed in the analogous phenyl radical + O_2 reaction system.

VI. Intramolecular Migration of the Methyl Group to the Peroxy Moiety of the 2-Methylphenylperoxy Radical (TS6). This reaction exhibits an activation energy 35 kcal mol^{-1} above the entrance channel and should therefore be of little importance. The transition states for the meta and para isomers should be even higher in energy and are not considered here.

VII. Addition of the Peroxy Radical at the Ortho Position in the 2-Methylphenylperoxy Radical (TS7 and TS8). This reaction leads to formation of the 4- and 6-methyl-5,6-dioxetane-2,4-cyclohexadienyl radicals. Activation energies for these reactions lie almost 10 kcal mol^{-1} below the entrance channel, and these intermediate radicals may therefore be of some importance, especially at higher temperatures.

3.4. Methylphenyl Radical + O_2 Kinetics. Rate constants have been determined for the chemically activated 2-methylphenyl radical + O_2 reaction system to products and stable intermediates as a function of temperature and pressure by the

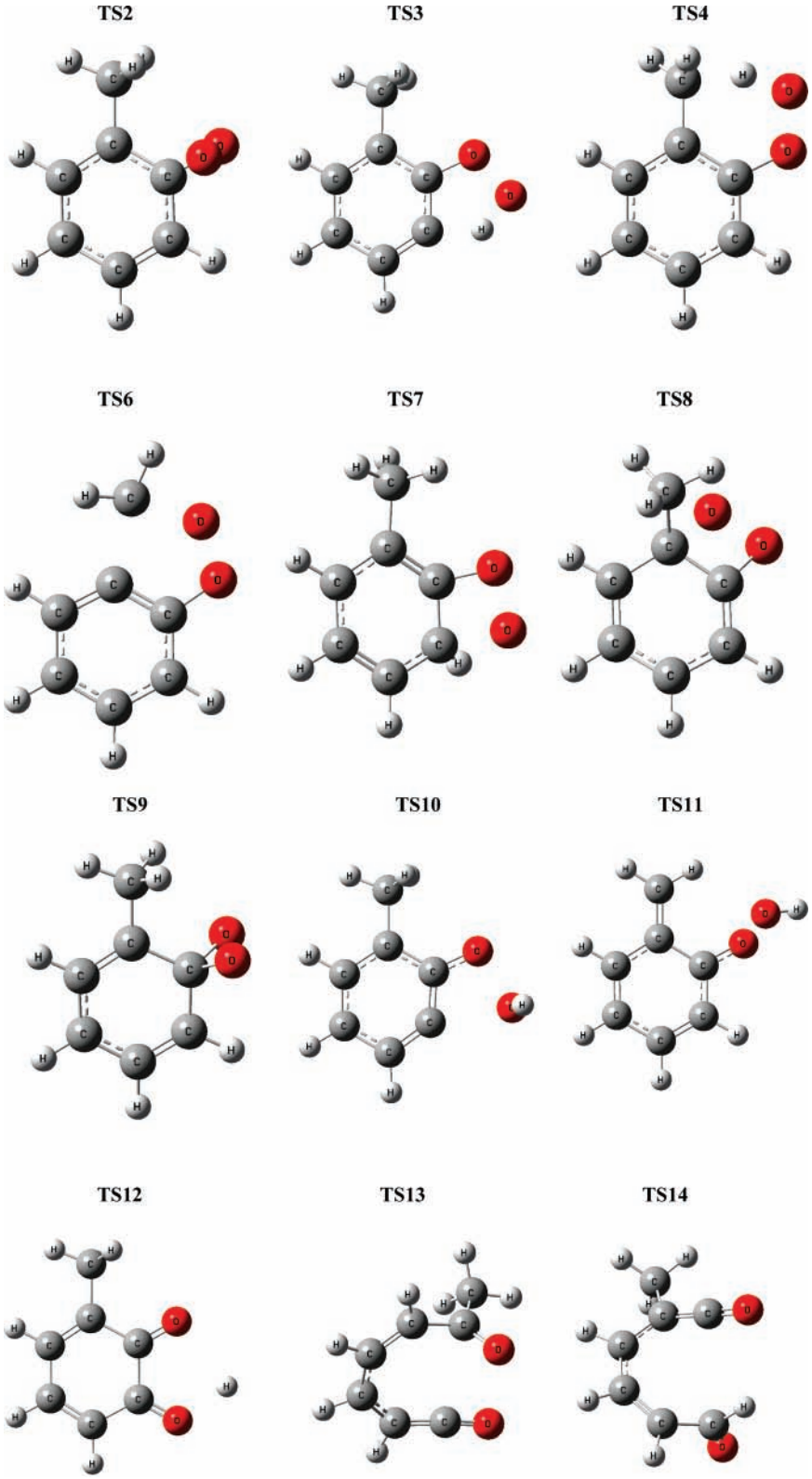

Figure 1. Geometries for all transition states identified in the 2-methylphenyl + O_2 reaction system at the B3LYP/6-31G(d) level.

qRRK/master equation analysis. Rate constants were obtained over a temperature and pressure range of 800−2400 K and 1 × 10^{-4} to 1000 atm. Analyses of the meta and para reaction systems were also analyzed by excluding the reaction pathways leading to *ortho*-quinone methide and the 2-methylperoxy-1-phenyl radical. Figures 3 and 4 show the respective rate constants as a function of temperature for chemical activation reactions of the 2-methylphenyl radical and the 4-methylphenyl radical reaction systems at 1 atm. The 2-methylphenyl + O_2 rate constants were found to be largely independent of pressure at higher temperatures, as illustrated in Figure 5. Rate constants for all three systems (i.e., ortho, meta, and para) at 800 ≤ T ≤ 2400 K and 0.0001 ≤ P ≤ 1000 atm are listed in the Supporting Information.

From our results, we find that the reactions leading to the methyloxepinoxy ring-opening products (the methyl-dioxo-hexadienyl radicals) in the 2-, 3-, and 4-methylphenyl + O_2 systems constitute the dominant pathways. These reactions

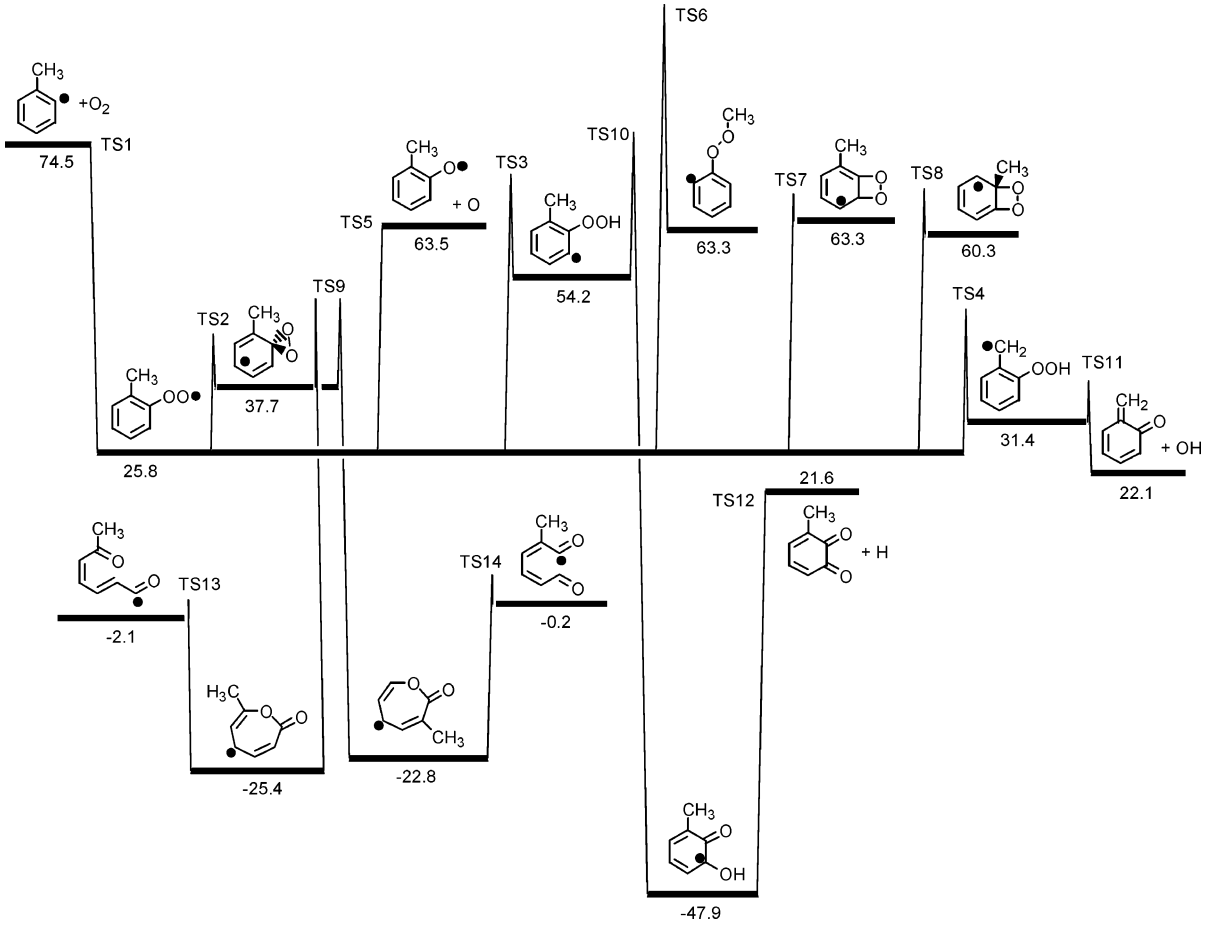

Figure 2. Potential energy diagram for reaction of the 2-methylphenyl radical with O_2. Enthalpies of formation ($\Delta_f H°_{298}$, kcal mol^{-1}) are average values from isodesmic G3 and G3B3 calculations.

TABLE 6: Recommended Enthalpies ($\Delta_f H°_{298}$), Entropies ($S°_{298}$), and Heat Capacities ($C_P(T)$) for Transition States Involved in the Methylphenyl Radical + O_2 Combustion Mechanism[a]

transition state[b]	$\Delta_f H°_{298}$	$S°_{298}$	$C_{P,300}$	$C_{P,400}$	$C_{P,500}$	$C_{P,600}$	$C_{P,800}$	$C_{P,1000}$	$C_{P,1500}$
TS2	46.9	89.84	30.31	38.93	46.30	52.29	61.13	67.26	76.29
TS3	70.6	90.36	30.87	39.63	47.09	53.17	62.12	68.23	77.02
TS4	52.3	84.77	30.70	40.08	47.92	54.18	63.23	69.33	78.06
TS6	109.7	87.51	31.82	40.58	47.93	53.86	62.59	68.65	77.55
TS7	66.5	88.93	29.74	38.54	46.02	52.09	61.04	67.23	76.32
TS8	65.9	87.55	29.85	38.79	46.30	52.34	61.20	67.32	76.33
TS9	51.9	90.08	30.65	39.27	46.61	52.56	61.34	67.42	76.39
TS10	77.7	92.33	32.45	40.87	47.91	53.58	61.94	67.75	76.43
TS11	39.0	92.50	33.34	42.03	49.19	54.87	63.13	68.84	77.39
TS12	21.6	94.78	33.83	41.90	48.77	54.41	62.84	68.69	77.22
TS13	1.0	95.84	33.30	41.10	47.70	53.14	61.43	67.35	76.28
TS14	7.0	97.51	33.28	40.79	47.31	52.78	61.19	67.22	76.28

[a] Geometries, frequencies, and moments of inertia from B3LYP/6-31G(d) calculations. Enthalpies in kcal mol^{-1}, entropies and heat capacities in cal mol^{-1} K^{-1}. [b] Transition states identified in Figures 2 and 3.

dominate at low to moderate temperatures and are competitive with methylphenoxy radical production at higher temperatures. Formation of the oxepinoxy radical is well-documented for the oxidation of benzene.[1d,e,42] The further reactions of oxepinoxy and its ring-opening product lead to formation of the cyclopentadienyl radical, 2,4-cyclopentadiene-1-one, and acetylene plus vinyl and formyl radicals. The reactions of the methyloxepinoxy radicals are discussed further in Section 3.8 of this study.

Figures 3 and 5 show that production of the 2-methylphenoxy radical + O is an important reaction pathway for the 2-methylphenyl + O_2 reaction at moderate to high temperatures, where it is competitive with the ring-opening reactions. Phenoxy radical production is also of similar importance in the reactions of the 3- and 4-methylphenyl radicals. It is well-known that the phenoxy radical decomposes to the cyclopentadienyl radical + CO,[43] and a similar reaction to the methylcyclopentadienyl radical is expected to occur for the methylphenoxy radicals. Additionally, there may be a lower energy pathway from the 2-methylphenoxy radical to 2-methylenephenol via an intramolecular hydrogen shift from the methyl group to the adjacent phenoxy oxygen atom. This species could then dissociate to *ortho*-quinone methide + H. This reaction is chain branching, producing *ortho*-quinone methide plus H and O atoms. Further study of the 2-, 3-, and 4-methylphenoxy radical reactions, as

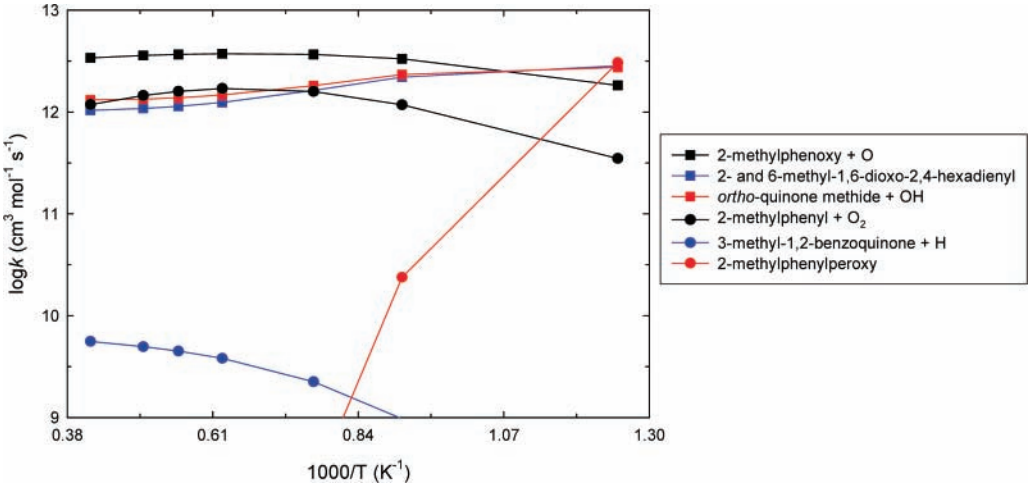

Figure 3. Rate constants (log(k)) as a function of temperature ($P = 1$ atm) for major products in the chemically activated 2-methylphenyl + O_2 system. The pathways to the two methyl-dioxo-hexadienyl radicals are plotted individually but proceed at the same rate.

TABLE 7: Elementary Rate Parameters (E_a, A', n) for Reactions on the 2-Methylphenyl Radical + O_2 Potential Energy Surface[a]

reaction[b]	E_a	A'	n
2-methylphenyl + O_2 → 2-methylphenylperoxy [TS1][c]	−0.71	3.72×10^{13}	−0.217
2-methylphenylperoxy → 2-methylphenyl + O_2 [TS1][c]	48.74	6.36×10^{19}	−1.372
2-methylphenylperoxy → 4-dioxirane-5-methyl-2,5-cyclohexadienyl [TS2]	21.1	5.89×10^{11}	0.193
2-methylphenylperoxy → 3-methyl-2-hydroperoxyphenyl [TS3]	44.8	5.04×10^{13}	−0.284
2-methylphenylperoxy → 2-phenylhydroperoxy-1-methylene [TS4][d]	26.5	1.58×10^{11}	0.352
2-methylphenylperoxy → 2-methylphenoxy + O [TS5][c]	38.54	1.27×10^{15}	−0.246
2-methylphenylperoxy → 2-methylperoxyphenyl [TS6][d]	83.9	2.82×10^{9}	0.933
2-methylphenylperoxy → 4-methyl-5,6-dioxetane-2,4-cyclohexadienyl [TS7]	40.7	5.33×10^{11}	0.122
2-methylphenylperoxy → 6-methyl-5,6-dioxetane-2,4-cyclohexadienyl [TS8]	40.1	1.71×10^{11}	0.201
4-dioxirane-5-methyl-2,5-cyclohexadienyl → 2-methylphenylperoxy [TS2]	9.2	4.99×10^{12}	0.031
4-dioxirane-5-methyl-2,5-cyclohexadienyl → 3-methyloxepinoxy [TS9]	14.2	3.03×10^{12}	0.141
4-dioxirane-5-methyl-2,5-cyclohexadienyl → 7-methyloxepinoxy [TS9]	14.2	3.03×10^{12}	0.141
3-methyl-2-hydroperoxyphenyl → 2-methylphenylperoxy [TS3]	16.3	3.14×10^{11}	0.074
3-methyl-2-hydroperoxyphenyl → 2-hydroxy-6-methylphenoxy [TS10]	23.5	1.04×10^{9}	1.029
2-phenylhydroperoxy-1-methylene → 2-methylphenylperoxy [TS4][d]	20.9	1.73×10^{12}	−0.134
2-phenylhydroperoxy-1-methylene → *ortho*-quinone methide + OH [TS11][d]	7.6	6.47×10^{12}	0.232
2-methylperoxyphenyl → 2-methylphenylperoxy [TS6]	46.3	1.54×10^{7}	1.249
4-methyl-5,6-dioxetane-2,4-cyclohexadienyl → 2-methylphenylperoxy [TS7]	3.2	1.16×10^{12}	0.075
6-methyl-5,6-dioxetane-2,4-cyclohexadienyl → 2-methylphenylperoxy [TS8]	5.6	1.81×10^{12}	0.031
2-hydroxy-6-methylphenoxy → 3-methyl-2-hydroperoxyphenyl [TS10]	125.7	1.40×10^{12}	0.616
2-hydroxy-6-methylphenoxy → 3-methyl-1,2-benzoquinone + H [TS12]	69.5	3.45×10^{11}	1.078
3-methyloxepinoxy → 4-dioxirane-5-methyl-2,5-cyclohexadienyl [TS9]	77.3	2.55×10^{11}	0.416
3-methyloxepinoxy → 6-methyl-1,6-dioxo-2,4-hexadienyl [TS13]	25.6	1.55×10^{12}	0.655
7-methyloxepinoxy → 4-dioxirane-5-methyl-2,5-cyclohexadienyl [TS9]	74.7	2.64×10^{11}	0.437
7-methyloxepinoxy → 2-methyl-1,6-dioxo-2,4-hexadienyl [TS14]	29.0	6.69×10^{12}	0.574

[a] High-pressure-limit rate parameters. E_a in kcal mol^{-1}, A' in cm^3 mol^{-1} s^{-1} (bimolecular), and s^{-1} (unimolecular). $k = A'T^n \exp(-E_a/RT)$. Calculated for $T = 300-2000$ K. [b] Transition states identified in Figures 1 and 2. [c] From ref 17. [d] Not present in the 3- and 4-methylphenyl + O_2 systems.

well as the reactions of the methylcyclopentadienyl radical, is required for toluene combustion and oxidation modeling.

For the 2-methylphenyl + O_2 system, the formation of *ortho*-quinone methide also constitutes an important reaction pathway; this reaction process is of comparable significance to the individual ring-opening pathways and the methylphenoxy + O atom channel. As noted, this *ortho*-quinone methide pathway is absent in the 3- and 4-methylphenyl + O_2 systems. Formation of *ortho*-quinone methide is chain propagating, with production of an OH radical. The OH radical rapidly abstracts C—H hydrogens due to the considerable strength of the HO—H bond (119 kcal mol^{-1}). The further reactions of *ortho*-quinone methide are discussed in Section 3.7 of this paper.

At lower temperatures (ca. 1000 K and below) and higher pressures, we find that formation of the stabilized methylphenylperoxy radical becomes important. The dissociation chemistry of this species needs to be considered in low-temperature oxidation systems such as in pre-ignition combustion and in cool flame combustion processes. These reactions are discussed below in Section 3.5. Stabilization of other non-ring-opening, parent radical intermediates is less important than the methylphenylperoxy radical, and their further reactions are not considered here.

Finally, formation of 3-, 4-, and 5-methyl-1,2-benzoquinone is a minor reaction pathway in the 2-, 3-, and 4-methylphenyl systems. The rate of methyl-benzoquinone formation is several orders of magnitude below that of the major products, and this does not constitute a significant reaction pathway. Not surprisingly, the high-energy pathways to 2-methylperoxyphenyl and methyl-dioxetane-cyclohexadienyl radicals are negligible at all temperature and pressure conditions examined.

3.5. Methylphenylperoxy Radical Dissociation Kinetics. Stabilization of the methylphenylperoxy radical is an important process in the reaction of the methylphenyl radical with O_2 at

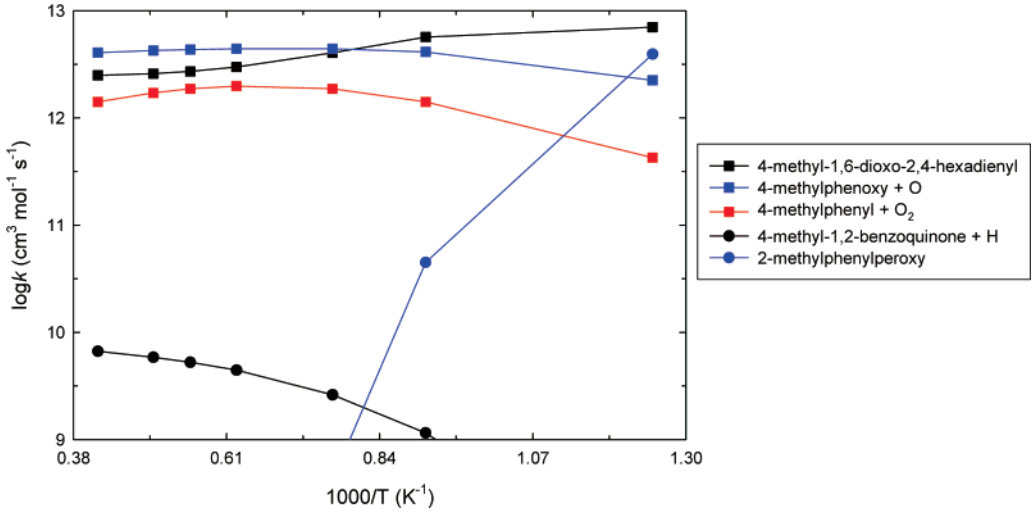

Figure 4. Rate constants (log(*k*)) as a function of temperature ($P = 1$ atm) for major products in the chemically activated 4-methylphenyl + O_2 system.

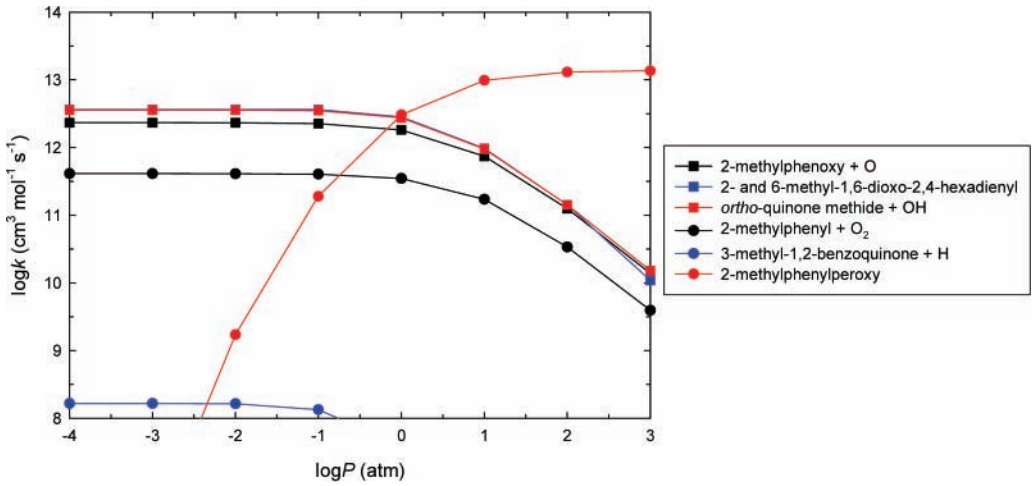

Figure 5. Rate constants (log(*k*)) as a function of pressure ($T = 800$ K) for major products in the chemically activated 2-methylphenyl + O_2 system. The pathways to the two methyl-dioxo-hexadienyl radicals are plotted individually but proceed at the same rate.

low temperatures and high pressures. We have modeled the kinetics of methylphenylperoxy isomerization and dissociation, where we included the same reaction pathways as for the chemically activated methylphenyl + O_2 reaction system (cf. Figure 2). Figure 6 shows branching ratios for dissociation and isomerization reactions in the 2-methylphenylperoxy radical system. The most important pathway for temperatures up to around 2000 K is the production of the two methyloxepinoxy ring-opening products (depicted in Figure 2 as the sum of the two pathways). *Ortho*-quinone methide is a major decomposition product at all examined temperatures, accounting for around 15−30% of the total reaction rate, and it is the second most important channel at temperatures below 1600 K. Formation of 2-methylphenoxy is also important, especially at temperatures of around 1200 K and greater, where it constitutes ca. 10−40% of the total reaction rate. The reverse dissociation reaction to methylphenyl + O_2 is only important at high temperatures, accounting for ca. 10% of the reaction rate at 1800 K and ca. 25% at 2400 K.

3.6. Kinetic Model Input. Rate parameters (A', n, E_a) for input to kinetic models are presented in Table 8 for the 2-methylphenyl + O_2 reaction system at 1 atm pressure. Rate parameters are for the important reaction pathways identified in the methylphenyl + O_2 chemically activated reaction and in the dissociation of stabilized methylphenylperoxy radicals.

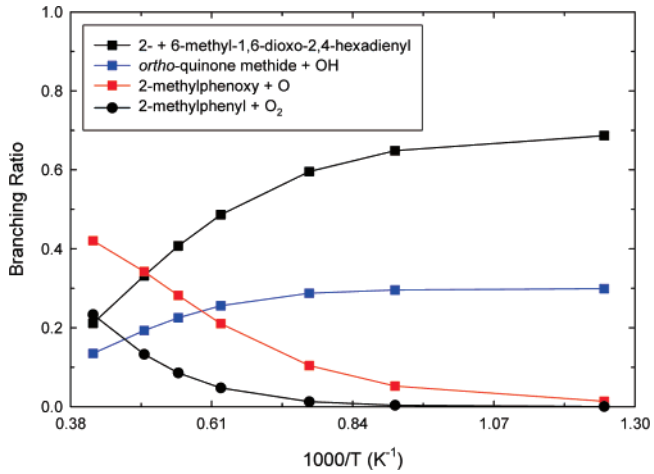

Figure 6. Branching ratios as a function of temperature ($P = 1$ atm) for major products in decomposition of the stabilized 2-methylphenylperoxy radical. The pathways to the two methyl-dioxo-hexadienyl radicals proceed at the same rate and are summed together.

Similar rate parameters for the 3- and 4-methylphenyl radicals are provided as Supporting Information, along with rate constants for all three systems as a function of pressure from 10^{-4} to 10^3 atm. It is hoped that improved modeling of toluene combustion can be achieved through the introduction of the

TABLE 8: Input Rate Parameters (E_a, A', n) for Use in Kinetic Modeling of the 2-Methylphenyl Radical + O_2 Reaction at P = 1 atm[a]

	A′	n	E_a
2-methylphenyl + O_2 → 2-methylphenylperoxy	3.21×10^{132}	−38.08	33.96
2-methylphenyl + O_2 → 2-methylphenoxy + O	9.18×10^{20}	−2.30	7.37
2-methylphenyl + O_2 → *ortho*-quinone methide	3.70×10^{12}	−0.18	−1.52
2-methylphenyl + O_2 → 2-methyl-1,6-dioxo-2,4-hexadienyl	5.59×10^{12}	−0.28	−1.94
2-methylphenyl + O_2 → 6-methyl-1,6-dioxo-2,4-hexadienyl	5.59×10^{12}	−0.28	−1.94
2-methylphenylperoxy → 2-methylphenyl + O_2	1.52×10^{34}	−6.56	48.79
2-methylphenylperoxy → 2-methylphenoxy + O	3.05×10^{37}	−7.61	43.66
2-methylphenylperoxy → *ortho*-quinone methide	2.03×10^{45}	−10.17	40.22
2-methylphenylperoxy → 2-methyl-1,6-dioxo-2,4-hexadienyl	9.46×10^{47}	−10.96	41.37
2-methylphenylperoxy → 6-methyl-1,6-dioxo-2,4-hexadienyl	9.65×10^{47}	−10.96	41.38

[a] E_a in kcal mol^{-1}, A' in cm^3 mol^{-1} s^{-1} (bimolecular) and s^{-1} (unimolecular). $k = A'T^n \exp(-E_a/RT)$. Valid for T = 800−2400 K.

SCHEME 4: Methyloxepinoxy Radicals and Their Ring Opening Products Formed in the Reactions of the 2-, 3-, and 4-Methylphenyl Radicals with O_2

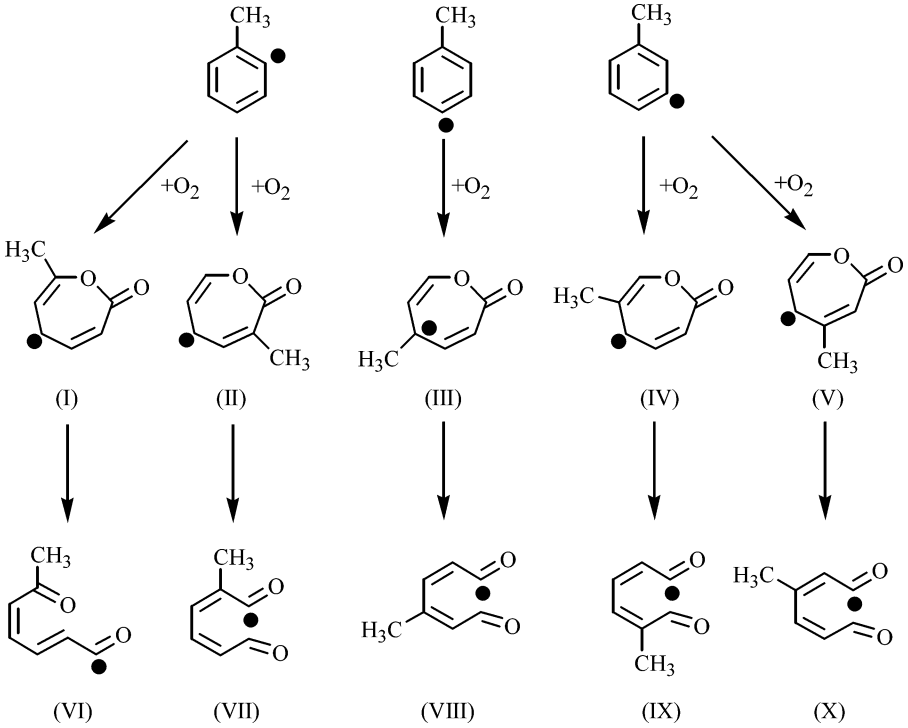

suggested rate parameters to existing combustion and oxidation mechanisms, along with rate constants for further reactions of the important intermediates and inclusion of a complete submechanism for benzene combustion.

3.7. *Ortho*-Quinone Methide. We have identified *ortho*-quinone methide as an important intermediate in the combustion reactions of toluene, and the further decomposition reactions of *ortho*-quinone methide need to be considered. The pyrolysis of *ortho*-quinone methide has been studied experimentally, as it is the primary decomposition product of chroman, an important model compound for lignin, which is found in wood and low-rank coals.[44] At temperatures of around 900 K and above, *ortho*-quinone methide rapidly pyrolyses to benzene + CO,[44] and the rate constant for this process is given as $6.31 \times 10^{14} \exp(-67.16/RT)$, in units of s^{-1} and kcal mol^{-1}.[44c] A minor pathway in *ortho*-quinone methide decomposition is the formation of fulvene + CO, which primarily decomposes to benzene, with some acetylene + 1-buten-3-yne. Stabilized *ortho*-quinone methide will also form *o*-cresol by the acquisition of two hydrogen atoms. A relatively large proportion of the activated *ortho*-quinone methide molecules produced from the 2-methylphenyl + O_2 reaction should possess enough chemical energy to undergo further decomposition.[45]

The above results reveal that *ortho*-quinone methide may serve as an important intermediate for the conversion of toluene to benzene in thermal oxidation and combustion processes. Interestingly, *ortho*-quinone methide is also a product in the reaction of the benzyl radical with HO_2, which should be important in the reaction of toluene in the atmosphere.[46] It is important to note that we predict the combustion of *ortho*-, *meta*- and *para*-xylene to result in formation of methyl *ortho*-quinone methide isomers, with subsequent decomposition to toluene. Abstraction of any one of the four phenyl hydrogen atoms in *para*-xylene will provide dimethylphenyl radicals that can all react with O_2 to yield methyl *o*-quinone methides. (We note that, for *ortho*- and *meta*-xylene, only two and three of the four isomeric dimethylphenyl radicals can lead to methyl *o*-quinone methide formation, respectively).

3.8. Methyloxepinoxy Radicals. The methyloxepinoxy radicals, and their ring-opening products (methyl-dioxo-hexadienyl radicals), are important products in the methylphenyl + O_2 association reactions, and detailed analysis of their unimolecular

SCHEME 5: Formation of Methylcyclopentadienyl + CO_2 from the Methyloxepinoxy Radical

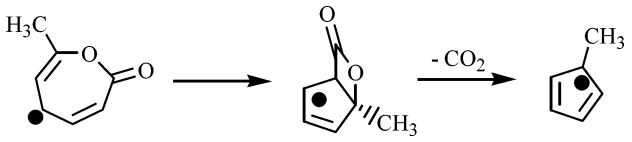

isomerization and dissociation reactions is warranted. Oxidation of the three methylphenyl radical isomers will result in the formation of the five isomeric ring-opening products depicted in Scheme 4. The methyloxepinoxy radicals (I) through (V) are: 3-, 7-, 5-, 4-, and 6-methyloxepinoxy, respectively. The ring opening products (VI) through (X) are: 6-, 2-, 4-, 5-, and 3-methyl-1,6-dioxo-2,4-hexadienyl, respectively. For oxidation of the 4-methylphenyl radical, we observe the formation of only 5-methyloxepinoxy (opening to 4-methyl-1,6-dioxo-2,4-hexadienyl). However, the overall rate of methyl-dioxo-hexadienyl radical formation will be the same, with two degenerate pathways for 5-methyloxepinoxy formation. Further complicating matters, the ring-opening products (VII) and (IX) and (VIII) and (X) are formed with sufficient energy to isomerize via an intramolecular hydrogen shift. The methyloxepinoxy radicals will also react to form the methylcyclopentadienyl radical via ring contraction followed by elimination of CO_2, as shown in Scheme 5. Here, the reaction products are independent of the location of the methyl group in the methyloxepinoxy radical.[1h] The stabilized methyloxepinoxy radicals are not observed to be significant products in either the chemically activated reaction of methylphenyl plus O_2 or the methylphenylperoxy dissociation reaction. Instead they serve as intermediates that rapidly isomerize or undergo ring opening and dissociate to new products. This is a result of the 98 kcal mol^{-1} in chemical activation energy that they are formed with from the initial reactants, or the ca. 75 kcal mol^{-1} energy from the transition state for isomerization of the stabilized methylphenylperoxy radical.

The ring-opening products (VI−X) formed in the methylphenyl + O_2 reaction will undergo a series of dissociation and cyclization reactions, forming new unsaturated products and five- and six-member ring compounds. These reactions are important, and similar to those of the 1,6-dioxo-2,4-hexadienyl radical, which is formed from ring opening of the oxepinoxy radical in the analogous benzene system.[47] Related reactions also take place in the oxidation of dibenzofuran.[47,48] For toluene, the ultimate products of this ring-opening pathway should include 2- and 3-methyl-2,4-cyclopentadiene-1-one, the methylcyclopentadienyl radical, acetylene, and the formyl and acetyl radicals. The reactions of these systems are the subject of a forthcoming article by our research group.

Many of the products formed by the further reactions of the methyl-dioxo-hexadienyl radicals, especially acetylene and the methylcyclopentadienyl radical, are important PAH/soot precursors. The acetyl radical is also an important product, as this radical rapidly dissociates to CH_3 and CO, with an activation energy of only 17 kcal mol^{-1}.[49] Methyl radicals under combustion conditions are active chain-propagating radicals, capable of abstracting benzyl, alkyl, and phenyl C−H hydrogen atoms. Production of the acetyl radical from methyloxepinoxy decomposition represents another potentially important reaction pathway not present in the analogous phenyl + O_2 or, indeed, in the benzyl + O_2, reaction mechanisms.

4. Conclusions

We have calculated thermochemical and kinetic parameters for reaction of the methylphenyl radical with O_2 in an effort to improve kinetic mechanisms describing the combustion of toluene, an important fuel component. We show that dialkyl-substituted benzenes react through methylbenzyl radicals to form alkyl-phenyl radicals, which will react similarly with O_2. A comprehensive reaction mechanism has been developed, featuring 16 species. Standard enthalpies of formation are determined for all species from G3 and G3B3 calculations by using isodesmic reaction schemes. Kinetic parameters are compiled for all reactions. A qRRK/master equation analysis is performed to determine rate constants as a function of temperature and pressure for the chemical activation and unimolecular dissociation reactions.

Our results suggest that the dominant reaction products in the chemically activated methylphenyl + O_2 systems are the methylphenoxy radicals + O and the methyl-dioxo-hexadienyl radicals formed upon ring opening. In the 2-methylphenyl + O_2 system, the production of *ortho*-quinone methide is also significant. Several important, new reaction paths are identified, and a number of the key paths are not considered in current models of toluene or alkyl benzene combustion. Reaction paths and kinetics are needed for a number of active intermediates, including the methyl-dioxo-hexadianyl radicals, which are identified as important initial products in this toluene oxidation system.

Acknowledgment. We acknowledge funding from ExxonMobil, the New Jersey Institute of Technology Ada C. Fritts Chair, and a U.S. Air Force Phase II STTR (contract number FA8650-06-C-2658). We thank the reviewers for their helpful comments.

Supporting Information Available: Calculated geometries (Cartesian coordinates), enthalpies (in hartrees), frequencies, and moments of inertia for all molecules and transition states. Internal rotor entropy and heat capacity corrections and C−CH_3 and C−OO internal rotor potentials. Recommended enthalpies of formation and uncertainties. Rate constants as a function of T and P for the reactions of 2-, 3-, and 4-methylphenyl radicals with O_2. Rate parameters (A', n, E_a) as a function of P for important pathways in the methylphenyl + O_2 reaction system. This material is available free of charge via the Internet at http://pubs.acs.org.

References and Notes

(1) (a) Chen, C.-C.; Bozzelli, J. W.; Farrell, J. T. *J. Phys. Chem. A* **2004**, *108*, 4632. (b) Tokmakov, I. V.; Kim, G.-S.; Kislov, V. V.; Mebel, A. M.; Lin, M. C. *J. Phys. Chem. A* **2005**, *109*, 6114. (c) Lindstedt, R. P.; Skevis, G. *Combust. Flame* **1994**, *99*, 551. (d) Merle, J. K.; Hadad, C. M. *J. Phys. Chem. A* **2004**, *108*, 8419. (e) Fadden, M. J.; Hadad, C. M. *J. Phys. Chem. A* **2000**, *104*, 8121. (f) Barckholtz, C.; Fadden, M. J.; Hadad, C. M. *J. Phys. Chem. A* **1999**, *103*, 8108. (g) Fadden, M. J.; Barckholtz, C.; Hadad, C. M. *J. Phys. Chem. A* **2000**, *104*, 3004. (h) Carpenter, B. K. *J. Am. Chem. Soc.* **1993**, *115*, 9806. (i) Mebel, A. M.; Lin, M. C. *J. Am. Chem. Soc.* **1994**, *116*, 9577.

(2) (a) Brezinsky, K.; Litzinger, T. A.; Glassman, I. *Int. J. Chem. Kinet.* **1984**, *16*, 1053. (b) Brezinsky, K.; Lovell, A. B.; Glassman, I. *Combust. Sci. Technol.* **1990**, *70*, 33. (c) Emdee, J. L.; Brezinsky, K.; Glassman, I. *J. Phys. Chem.* **1992**, *96*, 2151. (d) Griffiths, J. F.; Halford-Maw, P. A.; Rose, D. J. *Combust. Flame* **1993**, *95*, 291. (e) Roubaud, A.; Minetti, R.; Sochet, L. R. *Combust. Flame* **2000**, *121*, 535.

(3) (a) Pitz, W. J.; Seiser, R.; Bozzelli, J. W.; Seshadri, K.; Chen, C.-J.; Da Costa, I.; Fournet, R.; Billaud, F.; Battin-Leclerc, F.; Westbrook, C. K. *Proc. Combust. Inst.* **2004**, *30*. (b) Dagaut, P.; Pengloan, G.; Ristori, A. *Phys. Chem. Chem. Phys.* **2002**, *4*, 1846. (c) Pitz, W. J.; Seiser, R.; Bozzelli, J. W.; Da Costa, I.; Fournet, R.; Billaud, F.; Battin-Leclerc, F.; Seshadri, K.; Westbrook, C. K. *Fall Meeting, Western States Section of the Combustion Institute* **2001**, Paper 01F-28.

(4) (a) Gauthier, B. M.; Davidson, D. F.; Hanson, R. K. *Combust. Flame* **2004**, *139*, 300. (b) Andrae, J. C. G.; Björnbom, P.; Cracknell, R. F.; Kalghatgi, G. T. *Combust. Flame* **2007**, *149*, 2. (c) Herzler, J.; Fikri, M.; Hitzbleck, K.; Starke, R.; Schulz, C.; Roth, P.; Kalghatgi, G. T. *Combust. Flame* **2007**, *149*, 25. (d) Vanhove, G.; Petit, G.; Minetti, R. *Combust. Flame* **2006**, *145*, 521. (e) Andrae, J.; Johansson, D.; Björnbom, P.; Risberg, P.; Kalghatgi, G. *Combust. Flame* **2005**, *140*, 267. (f) Bounaceur, R.; Da Costa, I.; Fournet, R.; Billaud, F.; Battin-Leclerc, F. *Int. J. Chem. Kinet.* **2004**, *37*, 25.

(5) Yu, T.; Lin, M. C. *J. Am. Chem. Soc.* **1994**, *116*, 9571.

(6) Sebbar, N.; Bockhorn, H.; Bozzelli, J. W. *Phys. Chem. Chem Phys.* **2002**, *4*, 3691.

(7) Blanksby, S. J.; Ellison, G. B. *Acc. Chem. Res.* **2003**, *36*, 255.

(8) Oehlschlaeger, M. A.; Davidson, D. F.; Hanson, R. K. *J. Phys. Chem. A* **2006**, *110*, 6649.

(9) Oehlschlaeger, M. A.; Davidson, D. F.; Hanson, R. K. *Proc. Combust. Inst.* **2007**, *31*, 211.

(10) Hippler, H.; Reihs, C.; Troe, J. *Proc. Combust. Inst.* **1991**, *23*, 37.

(11) Frisch, M. J.; Trucks, G. W.; Schlegel, H. B.; Scuseria, G. E.; Robb, M. A.; Cheeseman, J. R.; Montgomery, J. A., Jr.; Vreven, T.; Kudin, K. N.; Burant, J. C.; Millam, J. M.; Iyengar, S. S.; Tomasi, J.; Barone, V.; Mennucci, B.; Cossi, M.; Scalmani, G.; Rega, N.; Petersson, G. A.; Nakatsuji, H.; Hada, M.; Ehara, M.; Toyota, K.; Fukuda, R.; Hasegawa, J.; Ishida, M.; Nakajima, T.; Honda, Y.; Kitao, O.; Nakai, H.; Klene, M.; Li, X.; Knox, J. E.; Hratchian, H. P.; Cross, J. B.; Bakken, V.; Adamo, C.; Jaramillo, J.; Gomperts, R.; Stratmann, R. E.; Yazyev, O.; Austin, A. J.; Cammi, R.; Pomelli, C.; Ochterski, J. W.; Ayala, P. Y.; Morokuma, K.; Voth, G. A.; Salvador, P.; Dannenberg, J. J.; Zakrzewski, V. G.; Dapprich, S.; Daniels, A. D.; Strain, M. C.; Farkas, O.; Malick, D. K.; Rabuck, A. D.; Raghavachari, K.; Foresman, J. B.; Ortiz, J. V.; Cui, Q.; Baboul, A. G.; Clifford, S.; Cioslowski, J.; Stefanov, B. B.; Liu, G.; Liashenko, A.; Piskorz, P.; Komaromi, I.; Martin, R. L.; Fox, D. J.; Keith, T.; Al-Laham, M. A.; Peng, C. Y.; Nanayakkara, A.; Challacombe, M.; Gill, P. M. W.; Johnson, B.; Chen, W.; Wong, M. W.; Gonzalez, C.; Pople, J. A. *Gaussian 03*, revision D.01; Gaussian, Inc.: Wallingford, CT, 2004.

(12) Curtiss, L. A.; Raghavachari, K.; Redfern, P. C.; Rassolov, V.; Pople, J. A. *J. Chem. Phys.* **1998**, *109*, 7764.

(13) Baboul, A. G.; Curtiss, L. A.; Redfern, P. C.; Raghavachari, K. *J. Chem. Phys.* **1999**, *110*, 7650.

(14) Wong, M. W.; Radom, L. *J. Phys. Chem.* **1995**, *99*, 8582.

(15) Sheng, C. Ph.D. Dissertation. New Jersey Institute of Technology, Newark, NJ, 2002; (program is available by e-mail to corresponding author).

(16) (a) Lay, T. H.; Krasnoperov, L. N.; Venanzi, C. A.; Bozzelli, J. W. *J. Phys. Chem.* **1996**, *100*, 8240. (b) Yamada, T.; Lay, T. H.; Bozzelli, J. W. *J. Phys. Chem. A* **1998**, *102*, 7286.

(17) da Silva, G.; Kim, C.-H.; Bozzelli, J. W. *J. Phys. Chem. A* **2006**, *110*, 792512.

(18) Sebbar, N.; Bozzelli, J. W.; Bockhorn, H. *J. Phys. Chem. A* **2004**, *108*, 8353.

(19) Wigner, E. P. *Z. Phys. Chem. B* **1932**, *19*, 203.

(20) da Silva, G.; Bozzelli, J. W. Unpublished material.

(21) Chang, A. Y.; Bozzelli, J. W.; Dean, A. M. *Z. Phys. Chem.* **2000**, *214*. 1533.

(22) Sheng, C.; Chang, A. Y.; Dean, A. M.; Bozzelli, J. W. *J. Phys. Chem. A* **2002**, *106*, 7276.

(23) Bozzelli, J. W.; Chang, A. Y.; Dean, A. M. *Int. J. Chem. Kinet.* **1997**, *29*, 161.

(24) Lee, J.; Chen, C.-J.; Bozzelli, J. W. *J. Phys. Chem. A* **2002**, *106*, 7155.

(25) Chase, M. W., Jr. *NIST-JANAF Thermochemical Tables*, 4th ed. *J. Phys. Chem. Ref. Data, Monograph*, **1998**, *9*, 1.

(26) Prosen, E. J.; Rossini, F. D. *J. Res. NBS* **1945**, 263.

(27) Prosen, E. J.; Gilmont, R.; Rossini, F. D. *J. Res. NBS* **1945**, *34*, 65.

(28) Tsang, W. Heats of Formation of Organic Free Radicals by Kinetic Methods. In *Energetics of Organic Free Radicals*; Martinho Simoes, J. A., Greenberg, A., Liebman, J. F., Eds.; Blackie Academic and Professional: London, 1996.

(29) Green, J. H. S. *Chem. Ind.* (*London*) **1960**, 1215.

(30) Khursan, S. L.; Martem'yanov, V. S. *Russ. J. Phys. Chem.* **1991**, *65*, 321.

(31) Roth, W. R.; Adamczak, O.; Breuckmann, R.; Lennartz, H.-W.; Boese, R. *Chem. Ber.* **1991**, *124*, 2499.

(32) Steele, W. V.; Chirico, R. D.; Nguyen, A.; Hossenlopp, I. A.; Smith, N. K. *AIChE Symp. Ser.* **1989**, *85*, 140.

(33) da Silva, G.; Sebbar, N.; Bozzelli, J. W.; Bockhorn, H. *ChemPhysChem* **2006**, *7*, 1119.

(34) Furuyama, S.; Golden, D. M.; Benson, S. W. *J. Chem. Thermodyn.* **1969**, *1*, 363.

(35) Prosen, E. J.; Maron, F. W.; Rossini, F. D. *J. Res. NBS* **1951**, *46*, 106.

(36) Cox, J. D. *Pure Appl. Chem.* **1961**, *2*, 125.

(37) Ruscik, B.; Pinzon, R. E.; Morton, M. L.; Srinivasan, N. K.; Su, M.-C.; Sutherland, J. W.; Michael, J. V. *J. Phys. Chem. A* **2006**, *110*, 6592.

(38) Desai, P. D.; Wilhoit, R. C.; Zwolinski, B. J. *J. Chem. Eng. Data* **1968**, *13*, 334.

(39) (a) Lay, T. H.; Bozzelli, J. W. *J. Phys. Chem. A* **1997**, *101*, 9505. (b) Sun, H.; Bozzelli, J. W. *J. Phys. Chem. A* **2001**, *105*, 4504. (c) da Silva, G.; Moore, E. E.; Bozzelli, J. W. *J. Phys. Chem. A* **2006**, *110*, 13979. (d) da Silva, G.; Bozzelli, J. W. *J. Phys. Chem. A* **2006**, *110*, 13058. (e) da Silva, G.; Bozzelli, J. W. *J. Phys. Chem. C* **2007**, *111*, 5760.

(40) Raghavachari, K.; Stefanov, B. B.; Curtiss, L. A. *J. Chem. Phys.* **1997**, *106*, 6764.

(41) da Silva, G.; Chen, C.-C.; Bozzelli, J. W. *Chem. Phys. Lett.* **2006**, *424*, 42.

(42) Kroner, S. M.; DeMatteo, M. P.; Hadad, C. M.; Carpenter, B. K. *J. Am. Chem. Soc.* **2005**, *127*, 7466.

(43) (a) Lovell, A. B.; Brezinsky, K.; Glassman, I. *Int. J. Chem. Kinet.* **1989**, *21*, 547. (b) Colussi, A. J.; Zabel, F.; Benson, S. W. *Int. J. Chem. Kinet.* **1977**, *9*, 161.

(44) (a) Dorrestijn, E.; Mulder, P. *J. Anal. Appl. Pyrolysis* **1998**, *44*, 167. (b) Dorrestijn, E.; Epema, O. J.; van Scheppinger, W. B.; Mulder, P. *J. Chem. Soc., Perkin Trans. 2* **1998**, 1173. (c) Dorrestijn, E.; Pugin, R.; Ciriano Nogales, M. V.; Mulder, P. *J. Org. Chem.* **1997**, *62*, 4804. (d) Britt, P. F.; Buchanan, A. C., III; Cooney, M. J.; Martineau, D. R. *J. Org. Chem.* **2000**, *65*, 1376.

(45) da Silva, G.; Bozzelli, J. W. *J. Phys. Chem. A* **2007**, *111*, 7987.

(46) Skokov, S.; Kazakov, A.; Dryer, F. L. *Fourth Joint Meeting of the U.S. Sections of the Combustion Institute*, Philadelphia, PA, March 20−23, 2005.

(47) (a) Sebbar, N.; Bockhorn, H.; Bozzelli, J. W. *Proc. Eur. Combust. Meet.* **2003**, 26. (b) Sebbar, N.; Bockhorn, H.; Bozzelli, J. W. *Int. J. Chem. Kinet.* **2007**, accepted for publication.

(48) Altarawneh, M.; Dlugogorski, B. Z.; Kennedy, E. M.; Mackie, J. C. *J. Phys. Chem. A* **2006**, *110*, 13560.

(49) Lee, J.; Bozzelli, J. W. *Int. J. Chem. Kinet.* **2003**, *35*, 20.